© 2019. Published by The Company of Biologists Ltd | Journal of Cell Science (2019) 132, jcs226183. doi:10.1242/jcs.226183

RESEARCH ARTICLE

Leishmania amazonensis hijacks host cell lysosomes involved in plasma membrane repair to induce invasion in fibroblasts

Victor Soares Cavalcante-Costa[1], Mariana Costa-Reginaldo[1], Thamires Queiroz-Oliveira[1], Anny C. S. Oliveira[2], Natália Fernanda Couto[2], Danielle Oliveira dos Anjos[3], Jane Lima-Santos[3], Luciana Oliveira Andrade[2], Maria Fátima Horta[1] and Thiago Castro-Gomes[1,*]

ABSTRACT

Intracellular parasites of the genus *Leishmania* are the causative agents of leishmaniasis. The disease is transmitted by the bite of a sand fly vector, which inoculates the parasite into the skin of mammalian hosts, including humans. During chronic infection the parasite lives and replicates inside phagocytic cells, notably the macrophages. An interesting, but overlooked finding, is that other cell types and even non-phagocytic cells have been found to be infected by *Leishmania* spp. Nevertheless, the mechanisms by which *Leishmania* invades such cells had not been previously studied. Here, we show that *L. amazonensis* can induce their own entry into fibroblasts independently of actin cytoskeleton activity, and, thus, through a mechanism that is distinct from phagocytosis. Invasion involves subversion of host cell functions, such as Ca^{2+} signaling and recruitment and exocytosis of host cell lysosomes involved in plasma membrane repair.

This article has an associated First Person interview with the first author of the paper.

KEY WORDS: Intracellular parasite, *Leishmania amazonensis*, Cell invasion, Lysosome, Plasma membrane repair

INTRODUCTION

The genus *Leishmania* comprises several species of intracellular parasites that cause a group of diseases collectively known as leishmaniasis. This parasitic infection is typical of tropical countries and occurs in several regions around the globe, affecting ∼14 million people and generating 1 million new cases each year (WHO Leishmaniasis, 2018, https://www.who.int/news-room/fact-sheets/detail/leishmaniasis; Burza et al., 2018). The disease is closely linked to poverty and is associated with malnutrition, population displacement, poor housing, immunosuppression and lack of financial resources. The outcome of the disease depends on the species and strain of the parasite, and on the immunological and nutritional status of the patient. The cutaneous form of leishmaniasis is commonly caused by the species *L. braziliensis*, *L. major* and *L. amazonensis*, and is characterized by the formation of skin lesions that can either heal spontaneously over time or evolve to a chronic condition, which can disseminate and lead to massive tissue damage. The most severe form of the disease is known as visceral leishmaniasis, commonly caused by the species *L. donovani* and *L. infantum*, which affects internal organs such as spleen and liver and is responsible for the majority of fatal cases.

Evolving a way to cross the host plasma membrane (PM) is a mandatory step for intracellular pathogens to establish infection. Therefore, a multitude of strategies to penetrate cells have been developed by different microorganisms. Cell invasion can be accomplished through formation of a moving junction that drives parasites into cells, as observed with the protozoans *Toxoplasma gondii* and *Plasmodium* spp. (Besteiro et al., 2011), direct injection of parasites through a specialized structure that punctures the PM as in microsporidians (Xu and Weiss, 2005), induction of phagocytosis as in *Leishmania*, *Listeria*, *Chlamydia* and others (Schille et al., 2018), or subversion of host cell endocytic pathways as in *Trypanosoma cruzi* (Fernandes et al., 2011). In the case of *Leishmania* spp., the parasite is transmitted through the bite of infected female phlebotomine hematophagous sand flies, which inject the flagellated infective promastigote forms into the mammalian host during blood meals. Once inside the mammalian host, promastigotes are ultimately captured by macrophages, which are considered to be their main host cells and in which parasites replicate as intracellular round-shaped forms, the amastigotes.

It has been reported that, before parasites reach macrophages, promastigotes are phagocytosed by neutrophils, the first immune cells to be recruited to the infection site a few minutes after inoculation into the dermis (Peters et al., 2008). Inside neutrophils, and already transformed into amastigotes, parasites are able to induce the apoptotic death of the host cell whose leishmania-containing apoptotic bodies are later captured by macrophages, which thereby become infected (Laskay et al., 2003; van Zandbergen et al., 2007). Because, in the lesions, amastigotes are mainly observed inside macrophages, these cells are the most studied and the best established infection model. However, cells unable to perform classical phagocytosis, such as fibroblasts, epithelial and muscle cells, have been reported to harbor *Leishmania* spp. amastigotes *in vitro* and *in vivo* (Bogdan et al., 2000; Minero et al., 2004; Holbrook and Palczuk, 1975; Schwartzman and Pearson, 1985; Schwartzman and Pearson, 1985). Despite its potential importance, the mechanism by which *Leishmania* spp. invade such cells remains elusive. Therefore, we sought to investigate how the parasite invades cells unable to perform classical phagocytosis using fibroblasts and *L. amazonensis* promastigotes as a model. Our results show that, *in vitro*, much like what is observed for the related trypanosomatid protozoan *T. cruzi*, *L. amazonensis* subverts the host cell endocytic pathway involved in plasma membrane repair, triggering Ca^{2+} signaling, lysosome-

[1]Departamento de Bioquímica e Imunologia, Instituto de Ciências Biológicas, Universidade Federal de Minas Gerais, Minas Gerais, CEP 31270-901, Brazil. [2]Departamento de Morfologia, Instituto de Ciências Biológicas, Universidade Federal de Minas Gerais, Minas Gerais, CEP 31270-901, Brazil. [3]Departamento de Ciências Biológicas, Universidade Estadual de Santa Cruz, Bahia, CEP 45662-900, Brazil.

*Author for correspondence (tcg@icb.ufmg.br)

V.S.C.-C., 0000-0003-2537-5514; M.C.-R., 0000-0002-7878-8833; T.Q.-O., 0000-0003-0306-0159; N.F.C., 0000-0003-0491-7062; T.C.-G., 0000-0003-1564-4645

Received 5 October 2018; Accepted 12 February 2019

Journal of Cell Science (2019) 132, jcs226183. doi:10.1242/jcs.226183

dependent recruitment and exocytosis to induce cell invasion in an actin cytoskeleton-independent fashion.

RESULTS

L. amazonensis invades MEFs *in vitro*

In order to verify whether *L. amazonensis* was able to invade mouse embryonic fibroblasts (MEFs), the cells were incubated with *L. amazonensis* parasites that express RFP (*LLa*-RFP) for 1 h and stained with phalloidin conjugated to Alexa Fluor 488 (phalloidin–AF488) and DAPI. Cells were analyzed by fluorescence microscopy using a Zeiss-Apotome microscope to obtain confocal images. In Fig. 1A, a 3D reconstruction including all *z* stacks obtained for an infected cell is shown, which displays the internalized parasite in the fibroblast (all stacks are provided in Fig. S1A). In Fig. 1B, a single focal plane of the same infected fibroblast shows a parasite (red) not colocalized with host cell F-actin (green), suggesting that invasion does not depend on actin cytoskeleton activity. Parasites were never observed colocalized with F-actin, which already suggested that cell entry does not need actin cytoskeleton activity (additional images of infected cells stained for F-actin are provided in Fig. S2A). To examine the kinetics of infection, we quantified the infection rate by performing flow cytometry. Fig. 1C shows that as early as 15 min after exposure, ∼18% of cells were RFP positive. From 30 min to 4 h there were no substantial changes, but after 24 h, ∼55% of the cells were infected. Since external parasites can be easily removed by trypsin treatment, we can assume that RFP-positive cells are the infected cells.

To verify whether host cell actin polymerization participates in the process of invasion, MEFs were pre-treated with cytochalasin D to inhibit actin polymerization, and infection was assessed. The result (Fig. 1D) shows not only that host cell actin polymerization is dispensable for cell invasion, but also that actin filament disassembly facilitates parasite entry, leading to an almost 4-fold increase in the infection rate. In order to determine whether invasion of MEFs is a unique property of metacyclic promastigotes, cells were incubated with either procyclic or metacyclic *LLa*-RFP promastigotes (Fig. 1E). We observed that, unlike metacyclic forms, procyclic promastigotes were not able to infect cells, indicating that the ability to invade MEFs is acquired during metacyclogenesis. To determine whether cell entry depended on the viability of parasites, MEFs were incubated with PFA-fixed or heat-treated *L. amazonensis*. We observed that, while the infection rate by living parasites reached 18% (4 h) and 56% (24 h), no PFA-fixed or heat-treated promastigotes were internalized by MEFs, apart from a negligible amount of heat-treated parasites at 24 h (Fig. 1F,G). This result shows that only living metacyclic promastigotes are able to enter MEFs.

In order to determine whether lysosomes fused with parasite-containing intracellular compartments, we stained cells with antibodies against the lysosomal protein LAMP2 and analyzed cells by fluorescence microscopy. Fig. 1H shows a single focal plane of an infected fibroblast harboring a parasite surrounded by LAMP2 (green) after 2 h of infection, demonstrating that the parasites are fully surrounded by a membrane containing the lysosomal marker LAMP2. Additional *z* stacks from this experiment are shown in Fig. S1B.

L. amazonensis persists and replicates within LAMP-containing vacuoles inside fibroblasts

In order to evaluate the fate of the parasites internalized in fibroblasts and their ability to replicate within the host cell, we analyzed the infected population by flow cytometry after 4 and 24 h of infection. Our results showed that the RFP mean fluorescence intensity of the infected population doubled at 24 h post infection, indicating that parasites were able to replicate inside fibroblasts (Fig. 2A). To evaluate whether parasites persist inside LAMP-containing vacuoles, we performed an immunofluorescence assay in which cells infected with *LLa*-RFP were fixed, labeled with anti-LAMP1 antibody and analyzed after 24 h of infection. Fig. 2B,C show two intracellular parasites with the typical amastigote morphology inside independent LAMP1-positive vacuoles in the perinuclear region of a single cell. This result shows that, upon uptake, *L. amazonensis* survives and is able to differentiate from metacyclic promastigotes into replicating amastigotes inside vacuoles with properties of lysosomes, similar to what occurs in macrophages. Images obtained by transmission electron microscopy (TEM) confirmed the presence of amastigotes within host cell parasitophorous vacuoles (PVs) (Fig. 2D, white and black asterisks). These images revealed the characteristic subpellicular microtubules (SMs) of *Leishmania* amastigotes, and a close juxtaposition between the parasitophorous vacuole membrane (PVM) and parasite membranes (Fig. 2E). After a week of infection, amastigotes were still observed inside single PVs (Fig. 2F), and the parasites showed no detectable alterations in their typical ultrastructural organization, including their nucleus (N), mitochondria (M) and flagellar pocket (FP) (Fig. 2G). After 10 days of infection, we could still observe cells containing viable amastigotes (Fig. 2H), as demonstrated by their ability to re-transform into flagellated promastigotes (Fig. 2I) after host cells were scraped off, inoculated into promastigote culture medium and incubated at 24°C for a week.

In vitro infection of fibroblasts by *L. amazonensis* involves Ca^{2+} signaling, plasma membrane permeabilization and lysosome recruitment/exocytosis

Cell invasion by intracellular parasites often involves Ca^{2+} signaling, which can induce changes in the PM that promote parasite entry (Pace et al., 1993; Valentin-Weigand et al., 1997; Dramsi and Cossart, 2003; Schettino et al., 1995; Fernandes et al., 2011). In order to evaluate whether *L. amazonensis* metacyclic promastigotes trigger Ca^{2+} signaling in fibroblasts, we loaded MEFs with the Fluo-4AM Ca^{2+} probe before inoculation of *LLa*-RFP and recorded fluorescence changes during the first 15 min of parasite–host cell contact. Intense intracellular Ca^{2+} transients were detected in fibroblasts (Fig. 3A,B; Movie 1) from the first minute of incubation and continued throughout the 15 min recording. Fig. 3B shows a quantification over time of the Fluo-4AM fluorescence intensity of each indicated cell, displayed as a graphical representation of the multiple Ca^{2+} transients induced in MEFs by contact with the *L. amazonensis* metacyclic promastigotes. To verify whether Ca^{2+} was flowing from the extracellular milieu to the cytoplasm through 'wounds' caused by the parasites on the PM, a monolayer of MEFs was incubated with *L. amazonensis* metacyclic promastigotes in the presence of propidium iodide (PI) and then analyzed by live fluorescence microscopy. We saw that, in the presence of parasites, some host cells become PI positive, showing that *L. amazonensis* promastigotes can induce PM permeabilization (Fig. 3C). When PI was only added at the end of the infection period and the cell population was analyzed by flow cytometry, we observed that 18% of the fibroblasts were stained by PI in the absence of Ca^{2+} (Fig. 3D). On the other hand, no significant PI staining was observed when cells were exposed to the parasites in the presence of Ca^{2+} (Fig. 3D), indicating that PM permeabilization is transient and that cells are able to recover when Ca^{2+} is present. To evaluate whether the presence of Ca^{2+} in the extracellular medium is important for parasite entry, we performed the infection assay in the presence of increasing concentrations of Ca^{2+}. The result (Fig. 3E) shows that while in low Ca^{2+} medium the infection is poor, the

Journal of Cell Science (2019) 132, jcs226183. doi:10.1242/jcs.226183

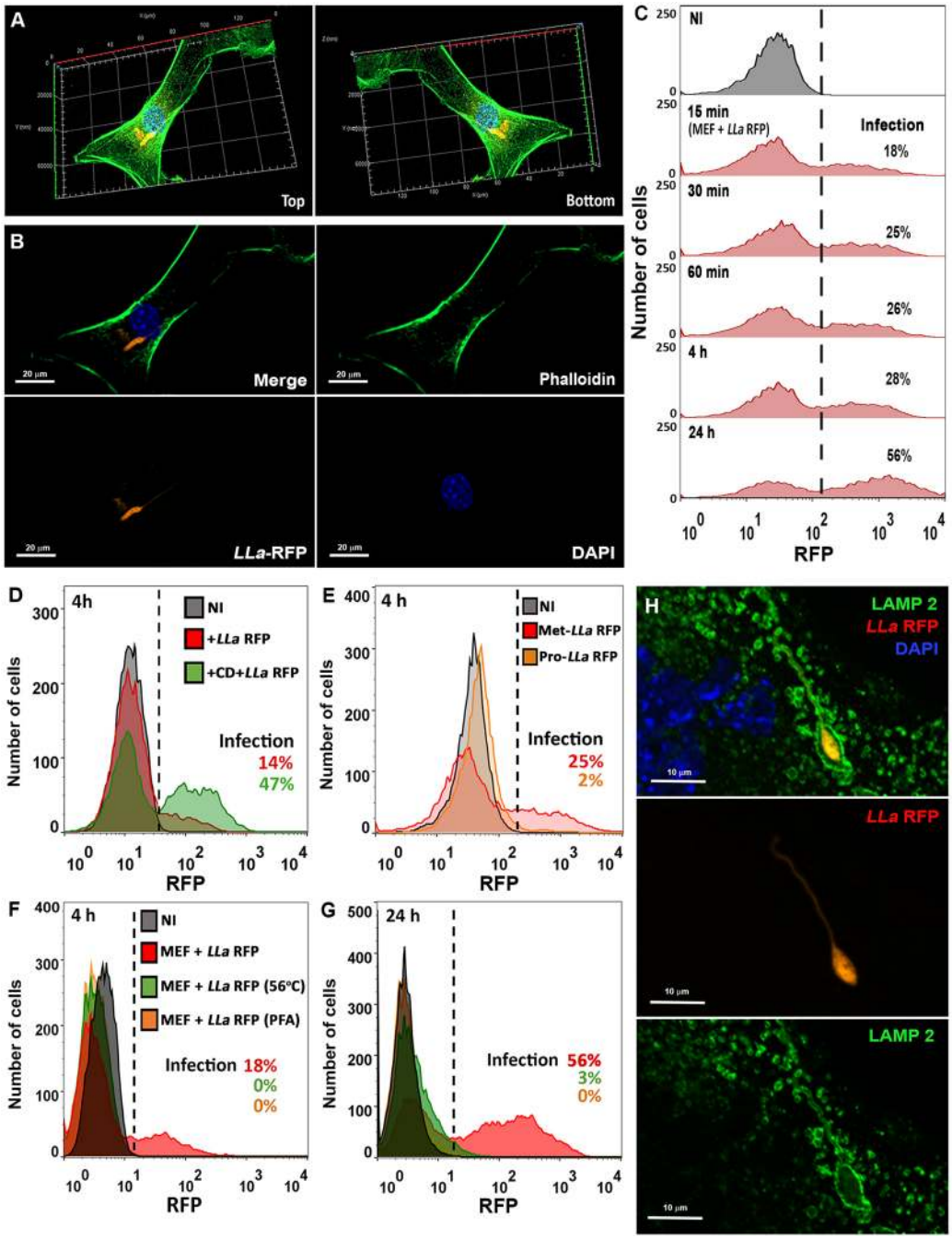

Fig. 1. Invasion of MEFs by *L. amazonensis in vitro* depends on parasite viability and infectivity and does not require host cell actin polymerization. (A) MEF infected by *L. amazonensis*. 3D reconstruction assembled from all *z*-stacks obtained from an infected MEF, displaying both sides of the infected cell. MEFs were incubated with *LLa*-RFP for 2 h at 37°C, labeled to visualize F-actin (green) and nuclei (blue) and imaged. (B) Single focal plane of the same infected fibroblast as in A showing that the parasite (red) is not colocalized with host cell F-actin (green). (C) Time course of MEF infection by *L. amazonensis*. Infection was performed as described in A; at the indicated time points cells were collected and infection quantified by means of FACS. Non-infected cells (NI) were gated as negative controls. (D) *L. amazonensis* infection of MEFs pre-treated with cytochalasin D (CD). MEFs were pre-treated (green) or not (red) with 10 µM CD for 15 min, infected with *LLa*-RFP for 4 h and infection was quantified by means of FACS. (E) MEF infection by procyclic or metacyclic promastigotes. MEFs were infected with *LLa*-RFP metacyclic (red) or procyclic (orange) promastigotes. Infection was performed and quantified as indicated in D. (F,G) MEF infection with live, PFA-fixed and heat-killed *LLa*-RFP metacyclic promastigotes. MEFs were incubated with live (red), heat-treated (green) or PFA-fixed (orange) *LLa*-RFP for 4 (F) or 24 h (G) and infection was quantified by means of FACS. (H) Infected MEF with host cell lysosomal staining. Cells were labeled by immunofluorescence to visualize lysosomes (green), nuclei (blue) and imaged using Axio Imager ApoTome2 Microscope (Zeiss) to obtain a single focal plane of a MEF infected with *LLa*-RFP (red) after 2 h of infection.

presence of free Ca^{2+} in the medium favors infection in a dose-dependent manner. Since Ca^{2+} transients could also be generated intracellularly by second messengers triggered by the contact with parasites, as previously shown for *T. cruzi* and other parasites (Tardieux et al., 1994), the same experiment as shown in Fig. 3A was performed in Ca^{2+}-free medium. As observed, parasites were able to trigger Ca^{2+} signaling even when Ca^{2+} was absent from the extracellular medium (Fig. 3F,G; Movie 2). Taken together, these

Journal of Cell Science (2019) 132, jcs226183. doi:10.1242/jcs.226183

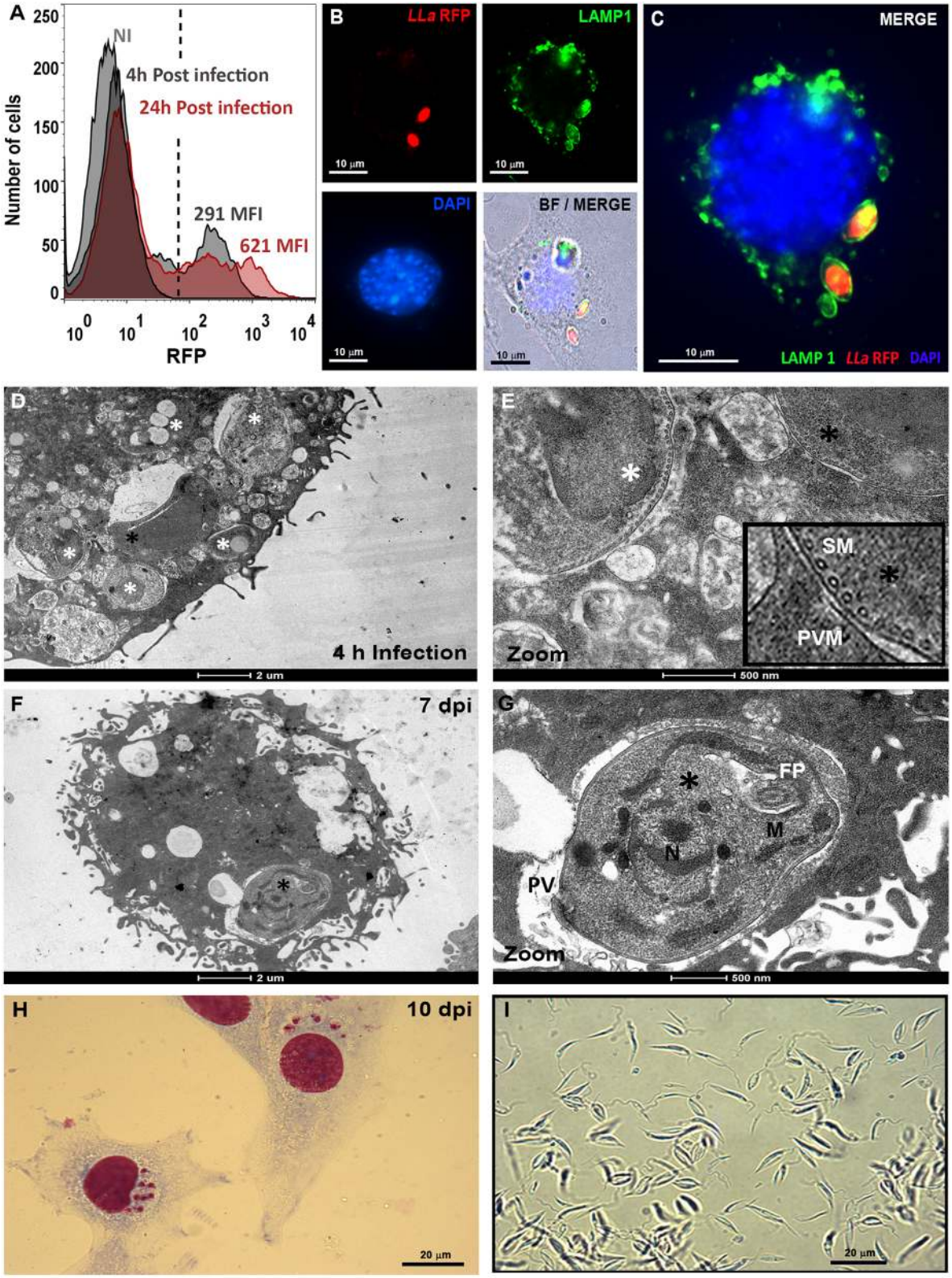

Fig. 2. See next page for legend.

results demonstrate that both intracellular Ca^{2+} signaling and extracellular Ca^{2+} influx occur during contact of *L. amazonensis* promastigotes and host fibroblasts.

One of the consequences of Ca^{2+} rising in the cytosol is the triggering of lysosomal exocytosis, an important step during the process of PM repair (Reddy et al., 2001). During this process, the exocytosis of lysosomes triggers the internalization of the wounded membrane by endocytosis (Tam et al., 2010), a process that can be subverted by endoparasites to invade cells (Fernandes et al., 2011). To assess whether the contact with parasites was affecting the

Journal of Cell Science (2019) 132, jcs226183. doi:10.1242/jcs.226183

Fig. 2. *L. amazonensis* resides in tight individual vacuoles rich in lysosomal markers and remains viable after differentiation into intracellular stages. (A) *L. amazonensis* replicate inside MEFs. After infection by *LLa*-RFP, the cell population was analyzed by FACS at 4 and 24 h post infection. The mean fluorescence intensity (MFI) of the infected population was calculated and is indicated for each curve. (B,C) *L. amazonensis* amastigotes residing in perinuclear vacuoles colocalized with lysosomal markers. MEFs were incubated with *LLa*-RFP for 24 h at 37°C, then labeled to visualize lysosomes (green) and nuclei (blue), and imaged using a BX60 upright compound fluorescence microscope (Olympus). The image shows each channel individually and also merged with (B) or without the bright field (BF) (C). (D–G) TEM analysis of MEFs infected with *L. amazonensis*. Cells were infected and prepared for electron microscopy after 4 h (D) or 7 days after infection (F). Asterisks show parasites inside MEFs. (E,G) Magnified images of the region indicated by a black asterisk in D and F, respectively. The insert in E shows a detail of the parasite PM with its typical subpellicular microtubules (SM) juxtaposed with the PVM. In G, an amastigote is shown within the PV with its flagellar pocket (FP), nuclei (N) and mitochondrion (M). (H) Hematoxylin-eosin staining of MEFs 10 days after infection. (I) Promastigotes obtained from MEF-derived amastigotes. The infected MEFs shown in H were scraped, inoculated into insect media and imaged 10 days later by conventional light microscopy.

distribution of host cell lysosomes, we incubated MEFs with infective promastigotes and labeled cells with anti-LAMP1 antibodies. The presence of parasites induced a noticeable redistribution of lysosomes towards the PM (Fig. 4A) and led to a significant increase of LAMP1 detection at cell periphery (Fig. 4C; additional images are shown in Fig. S3A,B). We also saw some images that suggest that host cell lysosomes are attracted and polarized towards parasite attachment site (Fig. 5; Fig. S2B). To verify whether lysosomes were also exocytosing their content upon contact *L. amazonensis*, MEFs were incubated with *LLa*-RFP and then labeled with anti-LAMP1 antibodies, this time without cell permeabilization. We observed that cells exposed luminal lysosomal protein epitopes on the extracellular leaflet of the PM (Fig. 4D; Fig. S3D), which is indicative of lysosomal exocytosis. Quantification by flow cytometry shows that ∼30% of cells incubated with live parasites exposed LAMP1 on their surface, an event not triggered by fixed parasites (Fig. 4E). Lysosomal exocytosis during cell entry was further confirmed by the detection of β-hexosaminidase enzymatic activity (Fig. 4F) and the presence of acid sphingomyelinase (ASM) and cathepsin-D (Fig. 4G) in culture supernatants during host cell exposure to living *L. amazonensis* promastigotes. In order to verify whether contact with parasites also enhanced endocytosis levels in MEFs, cells were labeled with wheat germ agglutinin (WGA)-conjugated Alexa Fluor 488, to stain the PM, and incubated with parasites for 15 min. After quenching the remaining extracellular fluorescence with Trypan Blue, the amount of endocytosed dye was quantified by flow cytometry. The result (Fig. 4H) shows that the presence of parasites increases endocytosis in MEFs, thus making cells more susceptible to invasion.

Since exocytosis of lysosomes is followed by a massive endocytosis (Idone et al., 2008) and generates ceramide-rich vacuoles (Fernandes et al., 2011) in an actin polymerization-independent manner, we decided to evaluate the presence of lysosomal markers and ceramide in vacuoles of recently internalized parasites. Cells were then infected with *LLa*-RFP for 1 h and labeled with anti-LAMP1 or anti-ceramide antibodies. As anticipated, parasites were completely surrounded by lysosomal markers (Fig. 4I) and ceramide (Fig. 4J; Fig. S3E) and both perfectly delineated bodies and flagella of the internalized metacyclic promastigotes. Conversely, and as previously stated, newly formed PVs were never covered by F-actin filaments (Fig. 1B; Fig. S2A). Taken together, these results indicate that the invasion process involves early lysosomal fusion and exocytosis, as previously demonstrated for *T. cruzi* (Tardieux et al., 1992).

Invasion of fibroblasts by *L. amazonensis* involves the recruitment of lysosomes to the infection site to form the nascent PV. In order to follow the recruitment of lysosomes to the parasite entry site, we carried out a time-course infection of MEFs by *LLa*-RFP, and prepared cells for fluorescence microscopy of anti-LAMP1 antibody staining. At 15 min of infection, we started to observe parasites closely interacting with fibroblasts and presenting an intense colocalization with LAMP1 at the flagellar portion (Fig. 5A). At 30–60 min of interaction, parasites were often observed with the flagella completely internalized and colocalized with lysosomal proteins while the parasite body seems to remain partially unlabeled (Fig. 5B). At 90 min, we observed parasites that were totally internalized, completely covered by the lysosomal marker and already located at the perinuclear region. At this point, we also started to observe the shortening of the flagella (Fig. 5C). From 120 min (Fig. 5D) to 24 h (Fig. 5E), parasites were found close to the nuclei inside a juxtaposed oval- or round-shaped vacuole, completely surrounded by the lysosomal protein and with no detectable flagella, in a typical amastigote morphology. To confirm that lysosomes are recruited at early steps of cell invasion and prior to complete parasite internalization, cells were labeled with anti-*L. amazonensis* LPG antibody to stain only the extracellular portions of invading parasites. Afterwards, cells were fixed and labeled with anti-LAMP1 antibodies to visualize host cell lysosomes. The results (Fig. 6A) show extracellular parasites totally stained by anti-LPG whereas recently internalized parasites were stained only by anti-LAMP1 antibodies (Fig. 6D). As suggested by the above results, the internalized portions of partially internalized parasites (Fig. 6B,C) merged with LAMP1, showing that lysosomes fuse with the PV as it forms. In Fig. 6C, we can see that whereas parasite bodies remain outside the host cell, and are thus labeled by anti-LPG antibodies (red), the internalized flagellar portion is totally delineated by the lysosomal marker (green, white arrow).

Lysosomal positioning and undamaged lysosomes are essential for fibroblast invasion by *L. amazonensis*

Lysosomes can be pre-linked to the PM at the cell periphery (Encarnação et al., 2016; Hissa et al., 2013) and associated with microtubules (Collot et al., 1984). In order to evaluate the role of microtubule-based movement of lysosomes in fibroblast invasion by *L. amazonensis*, we treated cells with the microtubule-blocking agent nocodazole before infection. There was no difference in invasion between cells treated or not with nocodazole (Fig. 7A), suggesting that PM-associated lysosomes might be sufficient to induce invasion. Cytochalasin D and brefeldin A are drugs known to lead to lysosome accumulation at the cell periphery (Tardieux et al., 1992). MEFs previously treated with each of these drugs showed a massive increase in infection by *L. amazonensis* (Fig. 7B,C). However, this increase was markedly blocked by nocodazole treatment (Fig. 7B,C). Cytochalasin D and brefeldin A treatment not only led to an increase in infected cells but also to a higher number of parasites per cell, as we could observe by fluorescence microscopy (Fig. 7D–F) and measure by flow cytometry, which showed an ∼2-fold increase in mean fluorescence intensity (data not shown).

Lysosomes are essential organelles whose exocytosis promotes the removal of PM lesions by endocytosis. To better evaluate the role of lysosomes in cell infection and specifically address whether PM repair is important for cell invasion, we performed

Journal of Cell Science (2019) 132, jcs226183. doi:10.1242/jcs.226183

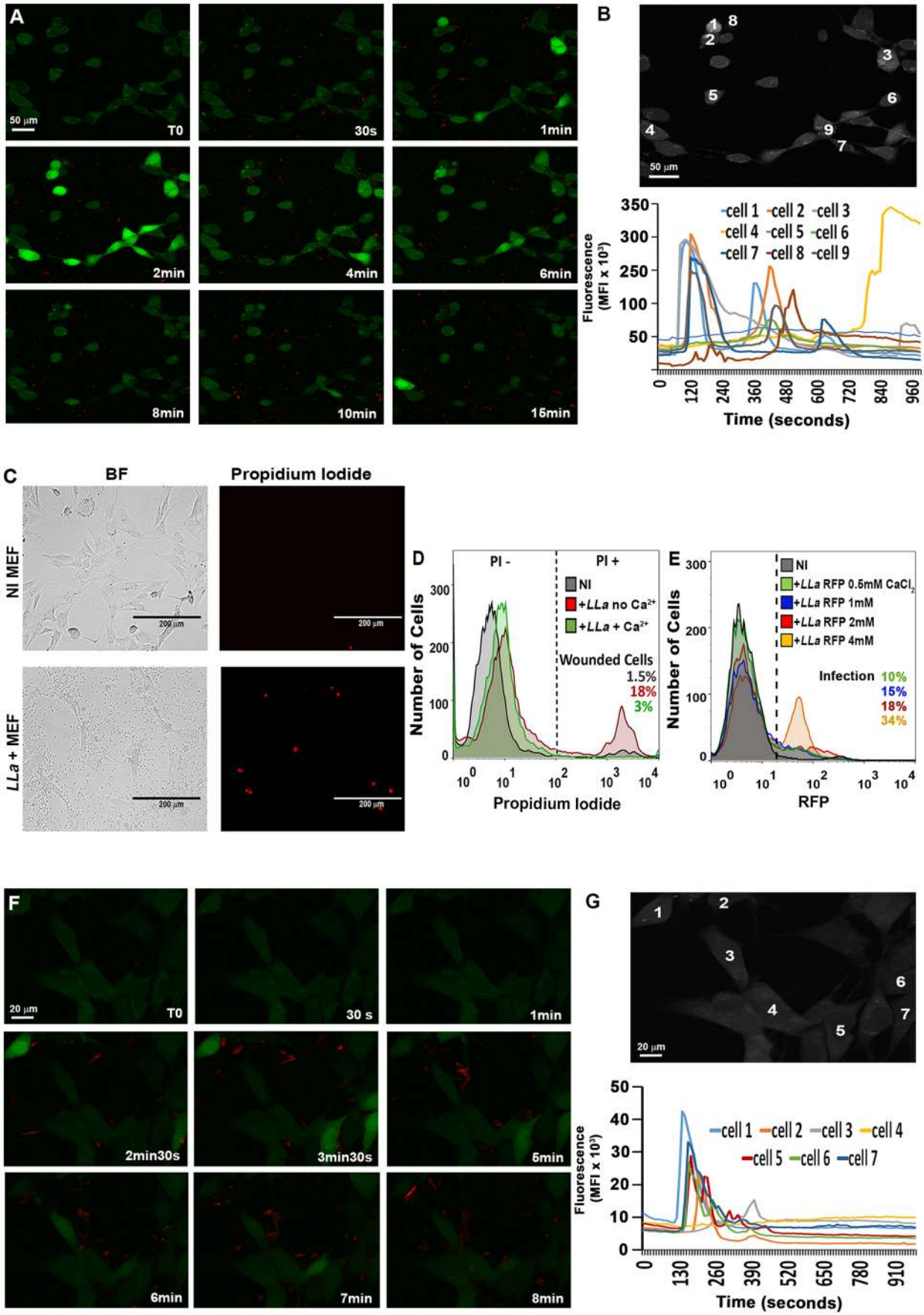

Fig. 3. See next page for legend.

Journal of Cell Science (2019) 132, jcs226183. doi:10.1242/jcs.226183

Fig. 3. Internalization of *L. amazonensis* in MEFs involves Ca^{2+} influx, PM permeabilization and intracellular Ca^{2+} signaling. (A) Visualization of Ca^{2+} fluxes induced by *L. amazonensis* in MEFs. MEFs were loaded with the Ca^{2+}-sensitive probe Fluo-4AM and incubated with *LLa*-RFP. Cells were imaged by live confocal microscopy at 10 frames/s. (B) Graphical representation of intracellular Ca^{2+} transients obtained from individual analysis of the nine indicated cells from the experiment shown in A. (C) Assessment of host cell PM permeability during *L. amazonensis* infection in MEFs. An MEF monolayer was incubated with *L. amazonensis* in the presence of propidium iodide (PI). After infection, the cells were examined by fluorescence microscopy. BF, bright-field image. (D) Quantification of cell permeability in MEFs during *L. amazonensis* infection in the presence or absence of Ca^{2+}. MEFs were incubated with *L. amazonensis* in the presence or absence of Ca^{2+} for 2 h. PI was added only at the end of the experiment and the cell population was analyzed by FACS. (E) Extracellular Ca^{2+} favors infection. MEFs were incubated with *LLa*-RFP with increasing concentrations of extracellular Ca^{2+} for 4 h and infection was quantified by FACS. NI, non-infected cells. (F) Detection of parasite-induced intracellular Ca^{2+} transients in MEFs. MEFs were loaded with the Ca^{2+} probe Fluo-4AM and incubated with *LLa*-RFP in the absence of extracellular Ca^{2+}. Cells were imaged by live confocal microscopy at 10 frames/s. (G) Graphical representation of intracellular Ca^{2+} transients obtained from individual analysis of 7 indicated cells from the experiment shown in in F. The movies from which the images in A, B, F and G are from are provided in supplementary information (A,B from Movie 1; F, G from Movie 2).

the *LLa*-RFP infection in LAMP2-knockout and LAMP1/2 double-knockout MEFs. These cells are known to be deficient in PM repair due to the accumulation of cholesterol and caveolin in lysosomes and, for this reason, are less susceptible to the invasion of *T. cruzi* (Couto et al., 2017). The results (Fig. 7G–I) show that the absence of these lysosomal proteins dramatically impairs *L. amazonensis* invasion.

Generation of transient PM wounds during parasite–host cell interaction increases invasion

Lysosome recruitment to cell periphery and lysosomal exocytosis are events that can be triggered by transient PM disruption. Ca^{2+} influx through, for example, streptolysin O (SLO) pores, leads to Ca^{2+}-dependent exocytosis of lysosomes, which is followed by a massive compensatory endocytosis that removes the damaged membrane from cell surface (Tam et al., 2010). Since we observed that parasites were inducing all these processes during cell entry, we decided to test whether inducing additional PM permeabilization during invasion would result in higher infection rates. First, we established an ideal concentration of SLO to obtain the maximum PM damage (in the absence of Ca^{2+}) with total cell recovery (in the presence of Ca^{2+}) (Fig. 8A). Cells started to become permeabilized (PI positive) at 50 ng/ml SLO, a concentration in which almost 100% of the cells were able to repair their PM (PI negative) (blue curves). When MEFs were treated with concentrations of SLO that allowed repair and concurrently incubated with *L. amazonensis*, infection of the cell population not only doubled (Fig. 8B) but the number of parasites/cell also increased, as observed through the ∼2-fold increase in the mean fluorescence intensity of each infected cell for both treatments (data not shown). The massive increase in invasion provoked by SLO treatment was also visualized when anti-LAMP1-labeled infected cells were analyzed by fluorescence microscopy (Fig. 8C–E). The results showed multi-infected cells (Fig. 8D) in which parasites also subsequently transformed into the replicating amastigote forms (Fig. 8E).

DISCUSSION

The remarkable ability of *Leishmania* spp. to survive and replicate inside phagocytes, such as neutrophils, macrophages and dendritic cells, has captured most of the attention and driven nearly all research in this field during the last decades. However, these parasites are also able to infect and survive in non-phagocytic cells, a feature already observed by several authors *in vitro* and *in vivo* (Bogdan et al., 2000; Rodríguez et al., 1996b; Schwartzman and Pearson, 1985; Holbrook and Palczuk, 1975) (reviewed by Rittig and Bogdan, 2000). In spite of the importance of such observations, almost no effort has been made to understand how these parasites succeed in infecting cells that are unable to perform classical phagocytosis. Here, using MEFs as a model, we show that entry of *L. amazonensis* into fibroblasts is a process that involves the ability of these parasites to actively induce a cell invasion mechanism involving transient PM permeabilization, Ca^{2+} signaling, lysosome recruitment/exocytosis and lysosome-triggered endocytosis, much like it has been established for another trypanosomatid, *T. cruzi* (Rodríguez et al., 1996a; Tardieux et al., 1992; Fernandes et al., 2011). Importantly, we demonstrate that this novel invasion mechanism by *L. amazonensis* is not a form of induced phagocytosis, since it does not seem to involve the host cell actin cytoskeleton.

While establishing assays for examining infection of MEFs by *L. amazonensis* promastigotes (Fig. 1A–C), it became evident that these cells could be invaded by the parasites, as these were found inside lysosome-derived vacuoles (Fig. 1H) as observed for macrophages. However, unlike the phagocytosis-mediated entry that occurs in macrophages, the invasion of MEFs by *L. amazonensis* depends on direct parasite activity, since PFA-fixed promastigotes and heat-treated parasites were not internalized (Fig. 1F,G). The conditions inside MEF PVs not only allowed the typical differentiation of promastigotes into amastigotes and their replication (Fig. 2A–C), but also the persistence of viable parasites (Fig. 2H,I), similar to what had been described for *L. donovani* in human fibroblasts (Schwartzman and Pearson, 1985).

Invasion of several intracellular microorganisms, such as *Salmonella typhimurium* (Pace et al., 1993), group B streptococci (Valentin-Weigand et al., 1997), *Listeria monocytogenes* (Dramsi and Cossart, 2003) and *T. cruzi* (Schettino et al., 1995; Fernandes et al., 2011), is accompanied by, or is dependent on, a rapid increase in the levels of free intracellular Ca^{2+}. In the model described here, contact with live *L. amazonensis* promastigotes also induced strong intracellular Ca^{2+} transients in MEFs (Fig. 3A,B,F,G). Ca^{2+} seems to be an important requirement for cell invasion by promastigotes, since its increase in the extracellular medium positively modulated parasite entry (Fig. 3E).

We then reasoned that one mechanism through which the parasites could trigger Ca^{2+} elevation in the cytoplasm might be via the generation of host cell PM wounds during invasion. Indeed, we showed that contact with live *L. amazonensis* promastigotes wounds the PM of host cells and that the lesions are promptly repaired in the presence of Ca^{2+} (Fig. 3C,D). In fact, when wounded, either by mechanical action or by pore-forming cytolysins, nucleated cells are able to reseal the PM in a process that involves Ca^{2+}-dependent exocytosis of lysosomes (Reddy et al., 2001). Secreted lysosomal enzymes have been proposed to act on the extracellular leaflet of the PM, triggering the removal of the wounded membrane through endocytosis (Tam et al., 2010; Andrews et al., 2015). Ca^{2+}-dependent exocytosis of lysosomes is followed by a wave of non-conventional endocytosis (Idone et al., 2008), which is used by parasites to invade non-phagocytic cells, as previously shown for *T. cruzi* (Fernandes et al., 2011). Thus, we hypothesized that host cell lysosomes are also essential for the infection of fibroblasts by *L. amazonensis*. Indeed, during infection of MEFs

Journal of Cell Science (2019) 132, jcs226183. doi:10.1242/jcs.226183

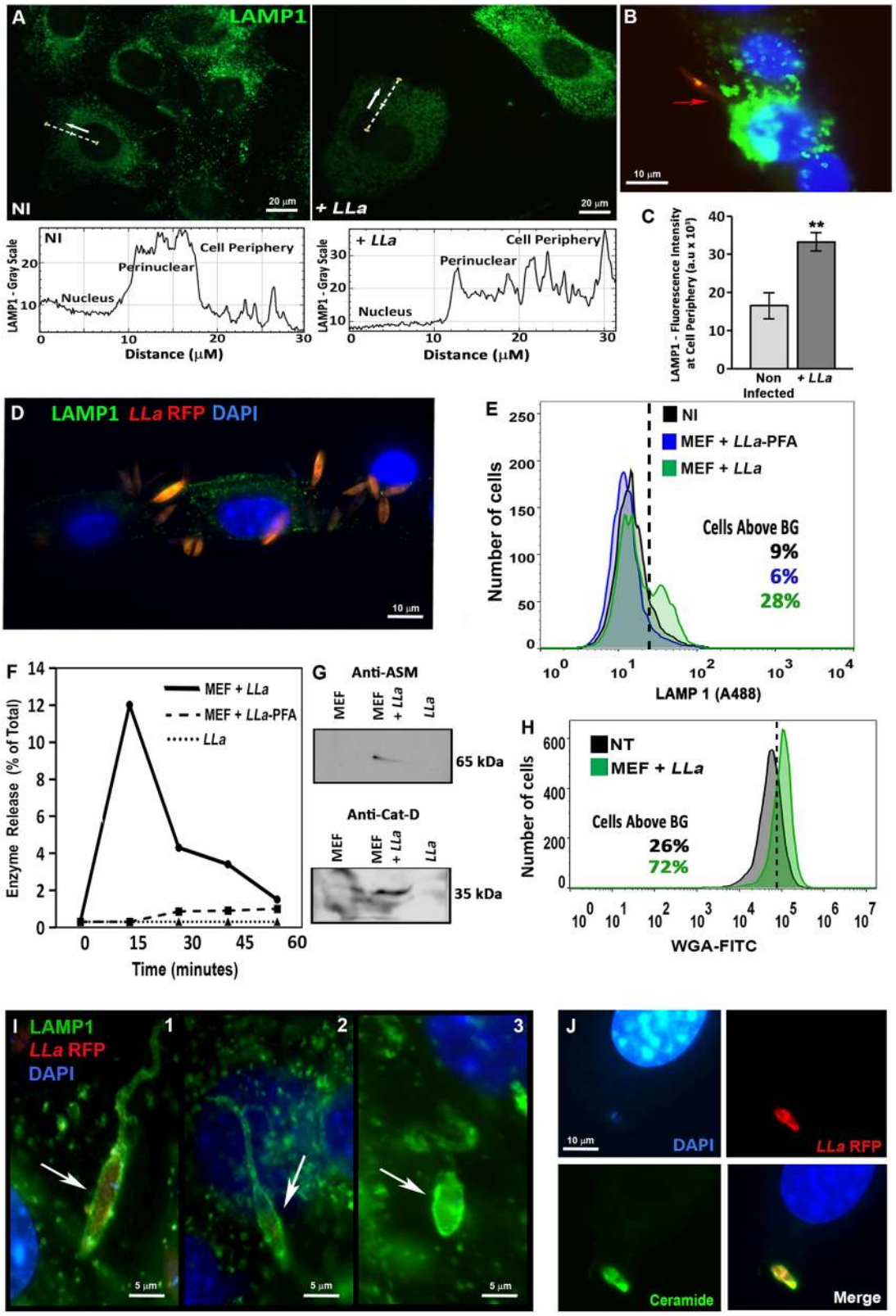

Fig. 4. See next page for legend.

with *L. amazonensis*, the presence of parasites induced a strong movement of host cell lysosomes towards the cell periphery (Fig. 4A,C), as well as lysosomal exocytosis (Fig. 4F,G) with a frequent accumulation of lysosomes at parasites attachment sites (Figs 4B and 5A; Fig. S2B). The exocytosis of lysosomes triggered by the parasites was followed by an increase in endocytosis levels in MEFs, indicating that the presence of parasites induces cell responses that facilitate invasion (Fig. 4H). Interestingly, recruitment of lysosomes to the infection site was observed from the very beginning of *L. amazonensis* interaction with MEFs (Fig. 5A;

Journal of Cell Science (2019) 132, jcs226183. doi:10.1242/jcs.226183

Fig. 4. *L. amazonensis* induces lysosomal exocytosis during cell entry in MEFs. (A–C) The contact with parasites induces the dispersion of lysosomes towards the cell periphery. MEFs were incubated with *LLa*-RFP for 30 min, and were then fixed and labeled to visualize lysosomes (green) (A). The fluorescence intensities were measured along lines drawn from the nucleus to cell edges (as indicated by the dashed lines in the image) and are represented in the graphs below each image. (B) Lysosomes were observed to accumulate at the invasion site (red arrow). (C) The fluorescence intensity of lysosomes harboring the cell periphery was quantified in cells as in B for each treatment. The data represent the mean±s.e.m. (NI, n=20; +*LLa*, n=12) $^{**}P$=0.0016, Student's t-test. (D) Exposure of LAMP1 on the extracellular leaflet of cells interacting with *L. amazonensis*. Same experiment as in A, but LAMP1 labeling was performed without cell permeabilization and before PFA fixation. (E) Quantification of lysosomal epitope exposure on the surface of MEFs incubated with live (blue) or PFA-fixed *L. amazonensis* (green) removed from the dish by scraping and directly analyzed by FACS. NI, non-infected cells. (F,G) Exocytosis of host cell lysosomal enzymes during *L. amazonensis* invasion in MEFs. (F) The activity of β-hexosaminidase was assayed in supernatants of cells incubated with living (solid line) and PFA-fixed *L. amazonensis* (dashed line). Controls with *L. amazonensis* alone were carried out (dotted line). (G) Supernatants were analyzed by western blotting using anti-ASM or anti-cathepsin D (Cat-D) antibodies. (H) Endocytosis quantification in MEFs incubated with *LLa*-RFP. MEF PM was labeled with Alexa-Fluor-488-conjugated WGA before incubation with parasites for 15 min. After parasite removal the extracellular fluorescence was quenched by Trypan Blue and the endocytosed dye was quantified by FACS. NT, non-treated cells. (I,J) Detection of LAMP1 and ceramide in recently formed *L. amazonensis* vacuoles. MEFs were infected with *LLa*-RFP for 1 h and labeled to visualize lysosomes (green) (I), ceramide (green) (J) and DAPI (blue) to stain nuclei, and imaged by using a BX60 upright compound fluorescence microscope (Olympus). White arrows (I) show recently internalized parasites.

Fig. S2B, 5 and 30 min). This was confirmed by identifying partially internalized parasites stained with anti-LPG antibodies, clearly showing that host cell lysosomes fuses with the PV as it forms, thus before the vacuole is pinched off from the host cell plasma membrane to the cytosol (Fig. 6). Notably, host cell PM wounding and exocytosis of lysosomes had already been observed in macrophages during *Leishmania* uptake by classical phagocytosis (Forestier et al., 2011), indicating that the mechanism described here may also be important during the invasion of phagocytes. However, in the case of macrophages, it was proposed that lysosomal fusion would be important to reseal PM wounds provoked by the movement of parasites after their internalization (Forestier et al., 2011). In the case presented here, exocytosis of lysosomes is an event triggered at early steps of the parasite–host cell interaction and culminates with parasite internalization. Interestingly, in the experiments described here the exocytosis of the lysosomal enzyme β-hexosaminidase peaked at 15 min of infection (Fig. 4F), matching the early triggering of Ca^{2+} transients (Fig. 3A) and the appearance of infected cells as early as 15 min after parasite inoculation (Fig. 1C). It is known that after exocytosis from lysosomes, ASM cleaves sphingomyelin on cell surface producing ceramide, a lipid that promotes negative curvature of the PM enabling endocytosis (Tam et al., 2010). A ceramide-rich vacuole, as opposed to actin-rich vacuole, is precisely what is observed in endosomes derived from the extracellular action of ASM during *T. cruzi* internalization (Fernandes et al., 2011). Also similar to earlier observations, we found that recently internalized *Leishmania* parasites are surrounded by a tight PV (Fig. 2E, insert), which is intensely stained by anti-LAMP1 (Fig. 4I) and anti-ceramide antibodies (Fig. 4J; Fig. S3E). This indicates that invasion actually takes advantage of exocytosis of lysosomes, which provide the membrane that allows parasite entry, in a mechanism that is markedly distinct from that of the classical parasite internalization that occurs through phagocytosis in macrophages. This is corroborated by the facts that *L. amazonensis* parasites can still invade MEFs pre-treated with cytochalasin D (Fig. 1D), and that recently internalized parasites do not colocalize with actin filaments (Fig. 1B; Fig. S2A). The involvement of lysosomes in the model of invasion described here was further confirmed by the fact that cytochalasin D and brefeldin A, two drugs that increase infection rates for *T. cruzi* by boosting the number of peripheral lysosomes, also increased the frequency of *L. amazonensis* infection in MEFs (Fig. 7B,C) and the number of parasites per cell, when compared to regular infection conditions (Fig. 7E,F). Since both effects could be prevented by treatment with nocodazole, a drug that destabilizes microtubules and stops lysosome traffic to cell periphery (Collot et al., 1984), we can infer that microtubule-associated lysosomes may play a role in infection. Interestingly, nocodazole could not prevent infection by itself, as observed for *T. cruzi* invasion (Tardieux et al., 1992), which is probably due to the fact that mammalian cells already have a portion of their lysosomes pre-bound to the PM, which could be sufficient to allow parasite invasion (Hissa et al., 2013). Moreover, LAMP2-knockout and LAMP1/2 double-knockout cells, which have modified lysosomes and impaired PM repair ability (Couto et al., 2017) are less susceptible to infection by *L. amazonensis* (Fig. 7H,I) than wild-type cells (Fig. 7G), similar to what was observed for *T. cruzi* infection with the same cell lines (Couto et al., 2017). Additionally, our results indicate that *Leishmania* promastigotes are able to trigger Ca^{2+} signaling in host cells from intracellular stores (Fig. 3F,G) since signaling also occurs in the absence of extracellular Ca^{2+}. Further investigation will be needed to identify the molecules involved in this signaling. However, regardless of the origin of the Ca^{2+}, from extracellular influx or intracellular reservoirs, the downstream effects important for cell invasion such as lysosomal exocytosis and its derived endocytosis would be triggered.

We still do not know how parasites induce PM injury in MEFs (Fig. 3C,D). However, at least two possibilities can be raised. First, that parasite movement against the host cell PM could generate mechanical wounds, as previously proposed for *T. cruzi* (Fernandes et al., 2011) and, second, that the parasites might secrete cytolytic molecules leading to PM permeabilization, as proposed for *Listeria monocytogenes* (Dramsi and Cossart, 2003). Since we have described that *Leishmania* spp. produce and secrete pore-forming cytolysins (Noronha et al., 2000; Castro-Gomes et al., 2009) it is possible that these molecules are responsible for permeabilizing host cells during invasion. Both possibilities would trigger Ca^{2+} influx, induce lysosome exocytosis and trigger endocytosis, playing a key role in promoting parasite invasion. Indeed, when additional PM wounding was induced in MEFs by adding the pore-forming protein SLO during *L. amazonensis* invasion, the frequency of infected MEFs doubled (Fig. 8A,B) and multi-infected cells appeared (Fig. 8D). When PM wounding was induced by SLO at the concentrations used (Fig. 8A), the host cells were able to reseal their PM, allowing the intracellular development of amastigote forms (Fig. 8E).

Although several authors have already reported the presence of *Leishmania* spp. amastigotes inside non-phagocytic cells *in vivo*, it is well established that, in chronic leishmaniasis, macrophages are the main cell type found to be parasitized. However, it has already been shown that macrophages may not be the primary cells infected at the bite site, as neutrophils (Peters et al., 2008) and dendritic cells (Bennett et al., 2001) are found to be infected by promastigotes, demonstrating that other cells may also be important to sustain the *Leishmania* life cycle. Given that the dermis, where parasites are inoculated, is rich in non-phagocytic cells, such as adipocytes,

Journal of Cell Science (2019) 132, jcs226183. doi:10.1242/jcs.226183

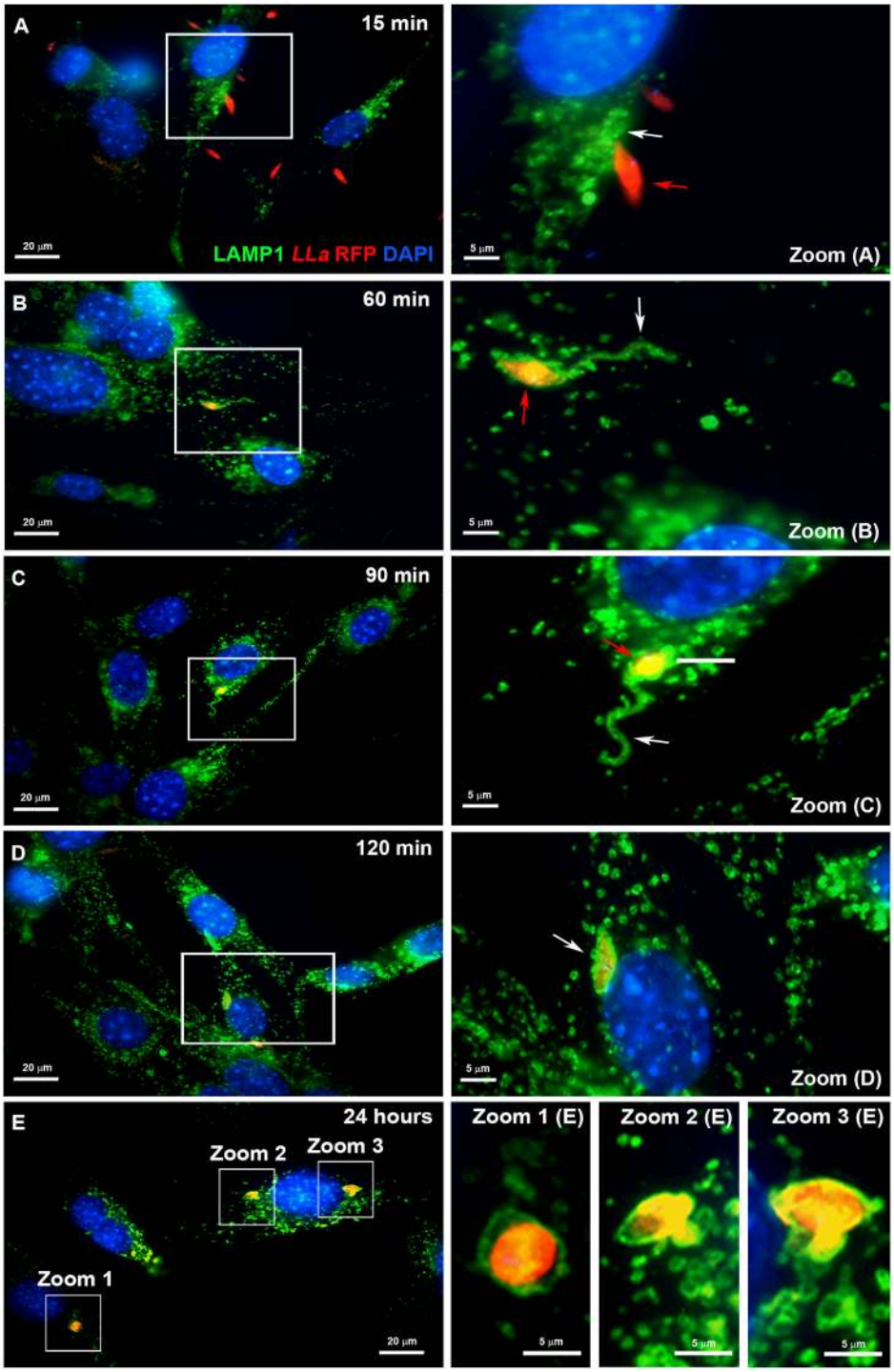

Fig. 5. Lysosomes accumulate at infection site in MEFs and envelop parasites as they gradually transform into intracellular amastigotes. MEFs were incubated with *LLa*-RFP (red). At the indicated time points, infection was stopped, cells were fixed, labeled to visualize lysosomes (green) and nuclei (blue), and imaged with a BX60 upright compound fluorescence microscope (Olympus). Each panel shows the merge of the three channels. (A) Lysosomal recruitment to infection site. (B) A partially labeled parasite with the flagella totally surrounded by the lysosomal marker LAMP1. (C) A completely internalized parasite located at the perinuclear region displaying flagellar shortening. (D) Internalized parasite presenting an ovoid form. (E) Typical amastigote forms within LAMP1-rich individual vacuoles at the perinuclear region. The white arrows indicate the flagellar region and the red arrows the parasite body. Magnified views (Zoom) of the indicated areas are shown on the right.

striated muscle cells, epithelial cells and fibroblasts, it is tempting to speculate that promastigotes may actively induce invasion of these cells *in vivo* through the mechanism described here.

Fibroblasts are actually interesting cells to consider during *in vivo Leishmania* infection, since they are the most abundant cells at the bite site, are major producers of chemokines that attract neutrophils and macrophages, directly interact with macrophages during wound healing and have the ability to move and spread through diapedesis (Smith et al., 1997; Shaw and Martin, 2016). In addition to the ability of *Leishmania* parasites to induce cell wounding and trigger endocytic repair responses, the phlebotomine vector bite site is known to be an area of intense tissue damage, largely caused by the vector proboscis that damages the surrounding tissue to increase blood supply. Thus, at the bite site, *Leishmania* parasites probably encounter several cell types that are undergoing PM repair, a process known to involve Ca^{2+} influx, lysosomal exocytosis, actin cytoskeleton rearrangements and endocytosis of wounded membranes. Besides providing a safe location to evade innate immunity, the rapid invasion of non-phagocytic cells shortly after inoculation would allow for a prompt transformation into amastigote forms, which could be later transferred to macrophages or serve as parasite reservoir. Transfer of amastigotes from an infected neutrophil to macrophages, known as the Trojan horse strategy, has been proposed to be a major mechanism allowing *in vivo* invasion of

Journal of Cell Science (2019) 132, jcs226183. doi:10.1242/jcs.226183

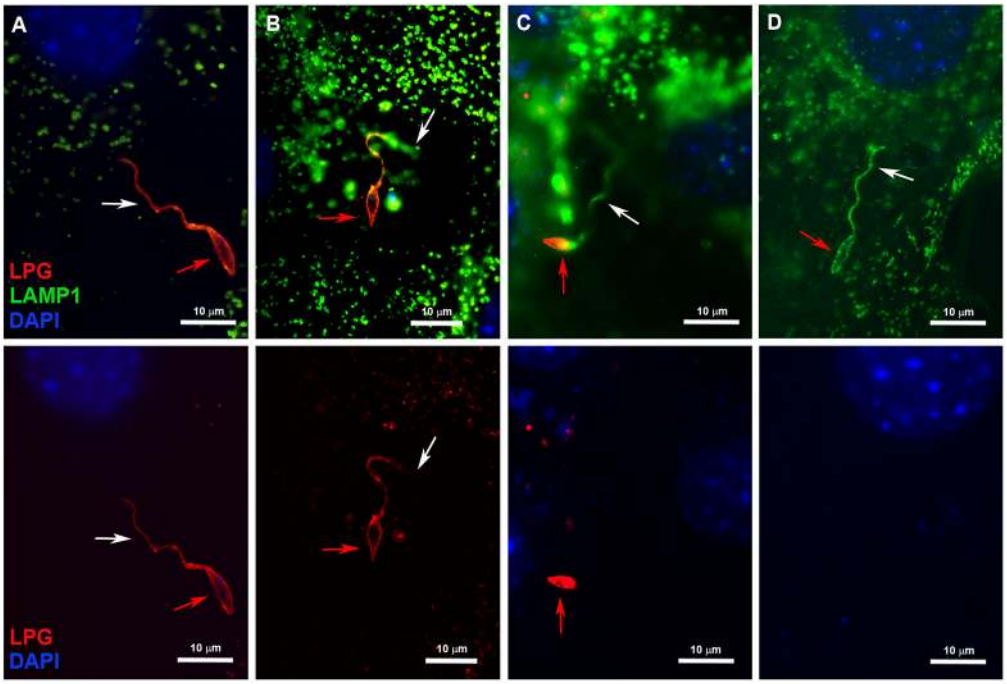

Fig. 6. Lysosomes are recruited at early steps of *L. amazonensis* infection in MEFs and envelop parasites as they gradually invade the host cell. (A–D) MEFs were incubated with metacyclic promastigotes of wild-type *L. amazonensis* for 60 min. In order to identify partially internalized parasites, the cells were labeled with anti-*L. amazonensis* LPG antibodies and secondarily marked with Alexa-Fluor-546-conjugated antibody (red), which stained only the extracellular portions of invading parasites. (A) An extracellular promastigote totally labeled (red). (B) A parasite partially internalized at the beginning of invasion by the flagellar tip shows LPG labeling (red) of the exposed extracellular portion whilst the internalized portion of the flagella merges with the lysosomal marker (green). (C) A parasite partially internalized at latter points of invasion shows an intense LPG labeling of the exposed cell body (red) whilst the internalized flagella merges and is tightly delineated by the lysosomal marker (green). (D) A recently internalized parasite totally protected from LPG staining. Red arrows, parasite body; white arrows, flagella. Cells were imaged using the BX60 upright compound fluorescence microscope (Olympus).

macrophages by *Leishmania* spp. (Laskay et al., 2003). In this context, it is possible that not only one, but several cell types could act as Trojan horses during *Leishmania* infection, notably at the early stages. Since these parasites are able to replicate inside fibroblasts *in vitro*, as we report here (Fig. 2A) and described by others (reviewed by Rittig and Bogdan, 2000), it is possible that a first round of replication inside these cells could be an important step leading to infection amplification, prior to macrophage invasion.

The ability to actively induce cell invasion characterized here is a neglected feature of *Leishmania* spp., probably due to the fact that these parasites have been largely perceived as passive players taken up by phagocytosis. *In vivo* experiments depicting the very first moments of natural infection are difficult to perform and have focused mainly on neutrophils and macrophages, not covering all cell types present at the infection site. Our findings emphasize the importance of performing more accurate and strictly controlled future investigations for characterizing all cell types harboring intracellular *Leishmania* during the first moments of natural infections and define their role in pathogenesis.

MATERIALS AND METHODS

Parasites and host cells

The PH8 (IFLA/BR/1967/PH8) strain of *Leishmania amazonensis* (*LLa*) used throughout this work was provided by Maria Norma Melo (Departamento de Parasitologia, Universidade Federal de Minas Gerais, Belo Horizonte, Brazil). Parasites were grown at 24°C in Schneider's Drosophila medium (Sigma) containing 10% heat-inactivated (hi) fetal bovine serum (FBS) (GIBCO), 100 U/ml penicillin and 100 µg/ml streptomycin (GIBCO). *L. amazonensis* expressing red fluorescent protein (*LLa*-RFP) were kindly provided by David Sacks (NIH, Bethesda, USA) and cultured as described by Carneiro et al., (2018). *LLa-RFP* promastigotes were grown as described for wild-type promastigotes with further addition of 50 µg/ml of geneticin G418 (Life Technologies), for selection of RFP-expressing parasites. Parasites were cultured for 4–6 days, a period in which cultures become enriched in infective metacyclic promastigotes. Metacyclic forms used in experiments were separated from procyclic forms using a Ficoll gradient, as described by Späth and Beverley (2001).

Mouse embryonic fibroblasts (MEFs), WT, LAMP2-knockout and LAMP1/2 double-knockout cell lines were obtained from Paul Saftig's laboratory (Biochemisches Institut/Christian-Albrechts-Universitat Kiel, Germany). Cells were cultured in DMEM (GIBCO) containing 10% hi FBS (GIBCO) at 37°C and in a 5% CO_2 atmosphere. Cultures were passaged every 48 h and plated, 24 h before experiments, on culture dishes (Sarstedt) or directly on glass coverslips, depending on the experiment. Sub-confluent cultures were used for infection experiments and were analyzed either by fluorescence microscopy or by flow cytometry. In the experiments described here, we used six-well dishes (Kasvi) and plated cells 24 h prior to experiments at 3×10^5 cells per well. For immunofluorescence analysis, round coverslips were placed on the well before cell platting. All cell lines used throughout this work were routinely tested for contamination and authentication.

Infection experiments

Purified *L. amazonensis* metacyclic promastigotes were used throughout the experiments, unless otherwise stated. Parasites were added to dish-adherent MEFs in DMEM containing 10% hi FBS (GIBCO) which were centrifuged at 500 ***g*** for 10 min at 15°C to synchronize parasite contact with cell monolayers, followed by incubation at 37°C in a 5% CO_2 atmosphere for the indicated periods of time. All experiments were performed using a multiplicity of infection (MOI) of 25 parasites per MEF. For some experiments, parasites were previously fixed in 4% PFA for 15 min or heat-inactivated for 30 min at 56°C.

Journal of Cell Science (2019) 132, jcs226183. doi:10.1242/jcs.226183

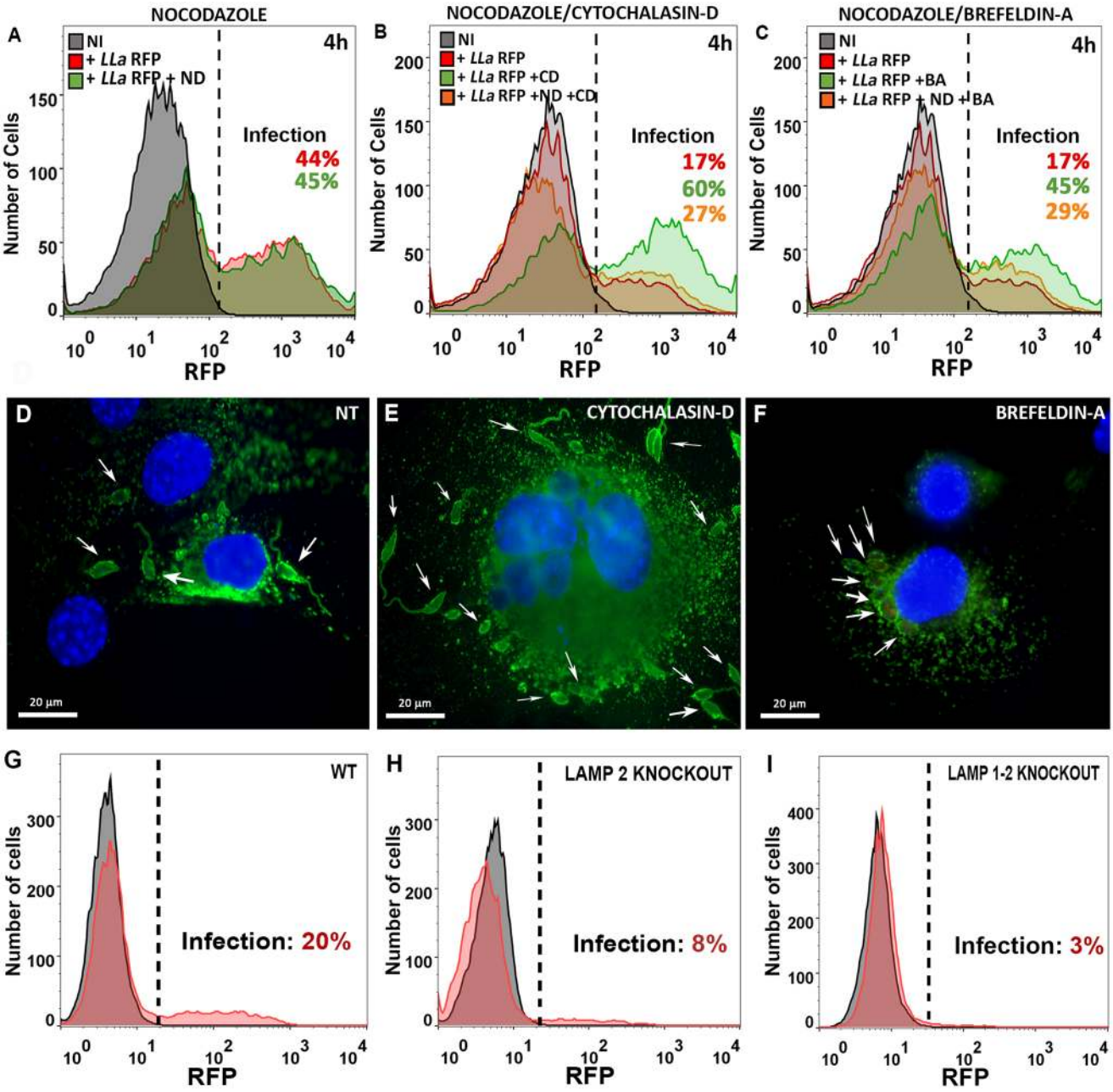

Fig. 7. Host cell lysosome positioning and lysosomal content are crucial for MEF invasion by *L. amazonensis*. (A) Role of host cell microtubules in the invasion of MEFs by *L. amazonensis*. MEFs were pre-treated with 20 µM nocodazole for 20 min; after drug removal cells were incubated with *LLa*-RFP for 4 h at 37°C and infection was quantified by FACS. (B,C) Cytochalasin D (CD) and brefeldin A (BA) treatment potentiates cell invasion in a microtubule-dependent manner. (B) MEFs were treated (orange) or not (green) with 20 µM nocodazole for 20 min prior to treatment with 10 µM cytochalasin D for 15 min, or (C) were treated (orange) or not (green) with 20 µM nocodazole for 20 min prior to treatment with 10 µM brefeldin A for 30 min. After drug removal, infection was performed as described for A and subjected to quantification by means of FACS. Infection of untreated MEFs by *LLa*-RFP is shown in red. NI, non-infected cells. (D–F) Multi-infected cells visualized after cytochalasin D and brefeldin A treatments. (D) Non-treated (NT) cells, (E) cytochalasin D pre-treated cells and (F) brefeldin A pre-treated cells were infected as described above, fixed, labeled to visualize lysosomes (green) and nuclei (blue), and imaged with a BX60 upright compound fluorescence microscope (Olympus). White arrows show internalized parasites. (G–I) Invasion of LAMP2-knockout and LAMP1/2 double-knockout MEFs by *L. amazonensis*. (G) Wild-type (WT), (H) LAMP2-knockout and (I) LAMP1/2 double-knockout MEFs were infected by *LLa*-RFP as described above and infection was quantified by FACS.

Cell labeling and western blotting

Immunofluorescence and fluorescent probes

Sub-confluent MEF monolayers were infected with *LLa*-RFP for the indicated periods of time and fixed with 4% paraformaldehyde. Preparations were blocked and permeabilized with PBS containing 2% BSA and 0.5% saponin and incubated with any of the following antibodies or compounds: rat anti-LAMP1 IgG (1:50, 1D4B), rat anti-LAMP2 IgG (1:50, ABL-93) (obtained from Developmental Studies Hybridoma Bank), mouse anti-ceramide IgM (1:50; C8104-50TST) (Sigma) or Alexa-Fluor-488-conjugated phalloidin (150 nM; Life Technologies). After washing, where appropriate, preparations were incubated for 30 min with Alexa- Fluor-488-conjugated equivalent secondary antibodies (Life Technologies). All preparations were stained with DAPI to visualize nuclei. Coverslips were mounted on microscope slides using anti-fading Prolong-Gold (Life Technologies) and analyzed by fluorescence microscopy. Images were acquired and analyzed using Q-Capture

Journal of Cell Science (2019) 132, jcs226183. doi:10.1242/jcs.226183

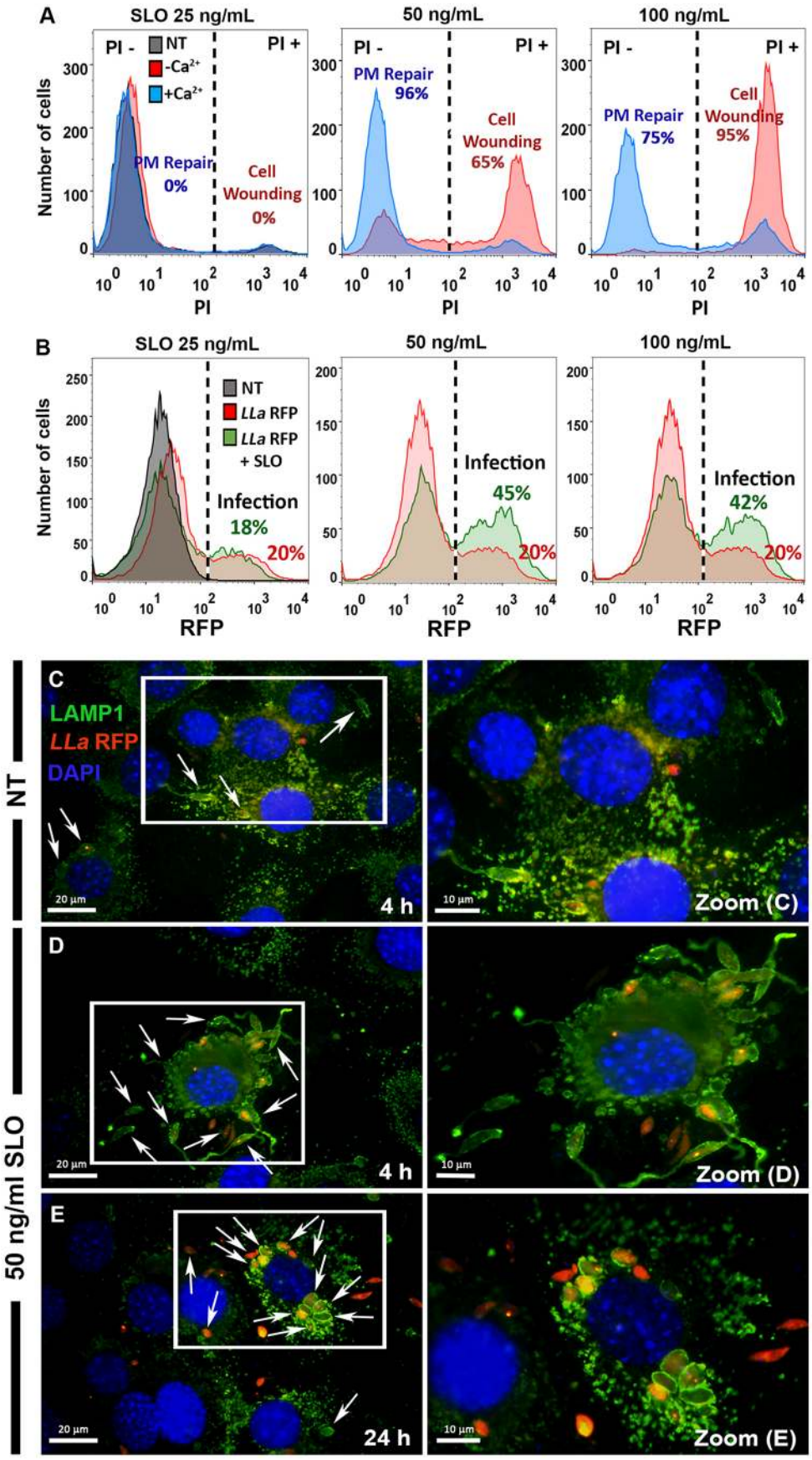

Fig. 8. Transient PM permeabilization enhances MEF invasion by *L. amazonensis*. (A) MEFs undergo PM repair in the presence of Ca^{2+}. MEFs were incubated with increasing concentrations of the pore-forming protein SLO at 37°C for 15 min in the presence or absence of Ca^{2+}. After the addition of PI, the cell population was analyzed by FACS. The percentages of cells showing 'wounding' (red) and cells that underwent PM repair (blue) are indicated in each graph. PM repair is indicated as the percentage of cells that excluded PI after being wounded by SLO. (B) Effect of SLO-triggered PM permeabilization on the invasion of MEFs by *L. amazonensis*. MEFs were incubated with *LLa*-RFP for 4 h. At 15 min of infection, SLO was inoculated into the medium at the indicated concentrations and infection was quantified by FACS. Infection of non-treated (red) and SLO-treated cells (green) is shown. The percentage of infection is indicated for each curve. (C–E) MEFs multi-infected by *L. amazonensis* after SLO-treatment. The experiment showed in Fig. 7B was carried out using 50 ng/ml SLO and cells were labeled to visualize lysosomes (green) and nuclei (blue) after 4 (C,D) or
24 h (E) of infection, and imaged with the BX60 upright compound fluorescence microscope (Olympus). White arrows show internalized parasites. Magnified views (Zoom) of the indicated areas are shown on the right.

software or Zen Software (ZEISS), depending on the experiment, as indicated. In order to evaluate the exposure of lysosomal epitopes on the PM by flow cytometry (FACS), cells were labeled as described above but without permeabilization or PFA fixation in order to detect only extracellular epitopes. For this purpose cells were removed from the dish with a cell scraper before analysis by FACS as described below.

L. amazonensis inside-outside labeling with anti-LPG antibodies

Sub-confluent MEFs were incubated with 25 parasites/cell for 60 min. In order to identify partially internalized parasites, the extracellular portions of promastigotes undergoing invasion were labeled without permeabilization with 1:400 mouse IgG anti-LPG (lipophosphoglycan), a major extracellular glycoconjugate epitope of *L. amazonensis*. The anti-LPG antibody (CA7AE) was kindly provided by Rodrigo Pinto Soares (Centro de Pesquisas René Rachou, Fundação Oswaldo Cruz, Brasil) and was produced as described by Soares et al., 2002. *L. amazonensis* LPG was secondarily labeled using 1:250 Alexa Fluor 546-conjugated antibody (Life Technologies) and cell nuclei were stained with DAPI. After LPG labeling and to visualize the recruitment of lysosomes to form the nascent PV, cells were permeabilized with PBS containing 2% BSA and 0.5% saponin, and labeled with anti-LAMP1 antibody (1D4B) and secondarily labeled with Alexa Fluor 488-conjugated antibody (Life Technologies) as described above.

Western blotting

Samples were prepared with reducing sample buffer, boiled for 5 min and fractionated by SDS-PAGE on 10% acrylamide gels (BioRad). After SDS-PAGE, proteins were transferred onto a nitrocellulose membrane using a wet transferring apparatus (BioRad). The membrane was blocked with 5% dry milk, followed by overnight incubation with 1:500 rabbit anti-acid sphingomyelinase (ASM) IgG (Abcam, ab83354) or goat anti-cathepsin-D IgG (Santa Cruz Biotechnology, sc-6486). After washing, membranes were incubated with the appropriate secondary antibody conjugated to horseradish peroxidase (HRP) (BioRad) at 1:10,000 in 5% dry milk for 1 h. After washing, the membrane was treated with Luminata HRP substrate (Milipore) and analyzed using a LAS-3000 imaging system (Fuji).

Quantification and visualization of infection

FACS

To quantify the rate of infections we took advantage of the *LLa*-RFP described above. After infection experiments, cells were washed, treated with 0.25% trypsin (Gibco) to detach cells and non-internalized parasites and then immediately analyzed the cell population by flow cytometry using a FACSCAN II (Becton Dickinson). All analyses took into account 10,000 events (MEFs) and were performed using Flow-Jo software.

Light microscopy

Visualization of infected cells was performed using BX60 Upright Compound Fluorescence Microscope (Olympus) after staining with a hematoxylin-eosin panoptic stain kit (RenyLab) and mounting on microscopy slides with Entellan (Merk). Images were obtained using Q-CapturePro Software.

Fluorescence microscopy

Cells labeled with fluorophore-conjugated antibodies or probes were analyzed with a BX60 Upright compound fluorescence microscope (Olympus) or Axio Imager ApoTome2 microscope (Zeiss) to obtain confocal images. In order to acquire single optical sections, *z* stacks were obtained in the ApoTome mode using structured illumination microscopy technology (SIM).

Transmission electron microscopy

MEFs infected with *L. amazonensis* promastigotes were fixed in 2.5% glutaraldehyde (Sigma) in 0.1 M sodium cacodylate buffer (pH 7.2) for 1 h at room temperature. Cells were then washed with 0.1 M sodium cacodylate buffer, collected with a scraper and post-fixed with a solution of 1% osmium tetroxide (O_sO_4) (Sigma), 0.8% potassium ferricyanide and 2.5 mM $CaCl_2$ for 1 h. After this second fixation step, cells were washed and dehydrated in a series ascending concentration of acetone (30–100%). Finally, cells were embedded in PolyBed resin at a ratio of 1:1 (acetone:resin) for 12 h, then in pure resin for 14 h, before being polymerized for 72 h at 60°C. Thin sections were obtained with diamond knives in an ultra-microtome (Leica UC7), collected on copper grids and stained in aqueous solutions of 6% uranyl acetate and 2% lead citrate for 30 and 5 min, respectively. Samples were observed with a Tecnai G2-20-SuperTwin FEI-200 kV transmission electron microscope.

Lysosome dispersion analysis

For lysosome dispersion analysis, we first established the perinuclear region, determined as oval-shaped areas around the nuclei with a small radius (0.5r) and a big radius (0.5R) (adapted from Nabavi et al., 2008 and as illustrated in Fig. S3C). Once the perinuclear region sizes were established, we quantified the fluorescence intensity of LAMP1–Alexa-Fluor-488-positive lysosomes inside this area. The fluorescence intensity of lysosomes at the cell periphery was obtained by measuring the whole-cell fluorescence and subtracting the fluorescence of the perinuclear region. The parasite-induced dispersion of lysosomes from the perinuclear region towards cell periphery was also represented by the intensity of LAMP1–Alexa-Fluor-488 fluorescence along a line drawn from the middle of cell nucleus to the edge of the cell. All images were analyzed using ImageJ software.

Evaluation of PM wounding and repair

The occurrence of PM wounding was evaluated by determining the degree of exclusion of the impermeant dye propidium iodide (PI), added to cell cultures at 50 µg/ml. PI-treated cells were analyzed by both fluorescence microscopy (EVOS) and flow cytometry. For fluorescence microscopy experiments using PI, MEFs were plated on six-well culture dishes and incubated with parasites in HBBS with or without Ca^{2+} in the presence of PI. To quantify PM wounding by means of flow cytometry, PI was added as indicated, cells were detached from plates with trypsin and analyzed by FACS.

Ca^{2+} signaling experiments

MEFs (1×10^5 cells per well) were platted in four-chamber glass bottom dishes and loaded with the Ca^{2+} probe Fluo 4 (Invitrogen) according to Luo et al., 2011, with slight modifications. Briefly, cells were washed twice with DMEM without FBS and incubated for 50 min with Fluo 4-AM loading solution (Invitrogen). Cells were then washed once with DMEM, three times with Ca^{2+}-free HBSS and maintained in HBSS containing or not containing 2 mM $CaCl_2$. Ca^{2+} transients were recorded by confocal video microscopy (Nikon C2) at 10 frames per second. At 40 s of imaging, 5 mM ionomycin (positive control), *LLa*-RFP or HBSS (negative control) were added to the medium and the videos were recorded for up to 15 min. Image analysis and quantification of fluorescence were performed using ImageJ and NIS Elements (Nikon) software.

Detection of lysosomal enzymes

MEF monolayers were incubated with *LLa* in RPMI without Phenol Red, and supernatants were analyzed for activity of the lysosomal enzyme β-hexosaminidase. At the indicated time points, supernatants were collected, centrifuged to remove detached cells and β-hexosaminidase activity was determined as described by Rodríguez et al. (1997). Briefly, 100 µl of each supernatant were incubated with 100 µl of 2 mM substrate 4-methyl-umbellyferyl-N-acetyl-b-d-glucosaminide (Sigma) in 6 mM citrate-phosphate buffer pH 4.5 for 15 min at 37°C. The reaction was stopped through addition of 25 µl of 2 M Na_2CO_3 and 1.1 mM glycine, and was read in a fluorimeter at excitation/emission wavelengths of 365/450 nm, respectively. The activity of β-hexosaminidase released in the supernatants is represented as the percentage of the total activity measured in the whole cell population. ASM and cathepsin D were detected by western blotting using anti-ASM or anti-cathepsin D antibodies, respectively, under reducing conditions and with samples prepared from FBS-free supernatants after 20 times concentration in a 10 kDa cutoff Amicon® centrifugal ultra-filter unit.

Endocytosis assay

In order to evaluate endocytosis triggered in MEFs by contact with *L. amazonensis*, 3×10^5 MEFs were plated in a six-well dish and the outer

leaflet of the PM was labeled with 1 µg/ml Alexa Fluor 488-conjugated wheat germ agglutinin (WGA) (Life Technologies) for 1 min at 4°C. Cells were then exposed or not to *L. amazonensis* promastigotes at 37°C for 15 min followed by treatment with 0.2% Trypan Blue (Sigma-Aldrich) for 2 min to quench the extracellular fluorescence. After washing, the cell population was removed from the dish by trypsin treatment and analyzed by FACS to detect the remaining cell-associated fluorescence corresponding to the endocytosed dye.

SLO and drug treatments

MEF monolayers were treated with 25, 50 or 100 ng/ml of the pore-forming protein SLO during infection, or 10 µM cytochalasin D (Sigma) for 15 min, or 10 µM brefeldin A for 30 min or 20 µM nocodazole for 15 min (Sigma). All drugs were added before infection and were removed from cells after incubation so as to not interfere with parasites viability. To evaluate plasma membrane repair triggered by SLO, fibroblasts were incubated with the indicated concentration of SLO in the absence of Ca^{2+} (non-repair condition) or after restoring Ca^{2+} with 2 mM $CaCl_2$ (repair condition) – after the addition of propidium iodide cells were analyzed by FACS.

Experimental repeat numbers

Each experiment in this manuscript was performed at least three times independently, the results show a typical example from one biological replicate. For infection experiments and FACS analysis, Fig. S6 shows the values of all the replicates performed. Where appropriate, the statistics (mean+s.d.) (graphs) or fold-increase values (tables) are also presented. Similarly, extra images and uncropped pictures are shown in the supplementary information as indicated in Figs S4 and S5.

Acknowledgements

We would like to thank Dr Norma Andrews for reagent donation, advice and critical reading of this manuscript, Dr Maria Norma Mello for proofreading this manuscript, Dr David Sacks for kindly providing RFP-expressing parasites, Dr Paul Saftig for kindly providing cell lines, Dr Rodrigo Pinto Soares for kindly providing the anti-LPG antibody used in this work, Elimar Faria for technical support, Jacob Kames and Rodrigo Silva Reston for professional English proofreading and manuscript editing. We also would like to thank CAPI (Centro de Aquisição e Processamento de Imagens) for all support with imaging and microscopy and the Flow Cytometry Laboratory-ICB-UFMG for support with all FACS analysis.

Competing interests

The authors declare no competing or financial interests.

Author contributions

Conceptualization: V.S.C.-C., T.C.-G.; Methodology: V.S.C.-C., M.C-R., T.Q.-O., A.C.S.O., N.F.C., D.O.d.A., J.L.-S., L.O.A., T.C.-G.; Validation: V.S.C.-C., M.C-R., T.Q.-O., A.C.S.O., N.F.C., D.O.d.A., J.L.-S., T.C.-G.; Formal analysis: V.S.C.-C., M.C.-R., A.C.S.O., N.F.C., D.O.d.A., J.L.-S., L.O.A., M.F.H., T.C.-G.; Investigation: V.S.C.-C., M.C-R., T.Q.-O., A.C.S.O., N.F.C., D.O.d.A., J.L.-S., M.F.H., T.C.-G.; Resources: M.F.H., T.C.-G.; Data curation: V.S.C.-C., M.C-R., A.C.S.O., N.F.C., D.O.d.A., J.L.-S., M.F.H., T.C.-G.; Writing - original draft: V.S.C.-C., T.C.-G.; Writing - review & editing: L.O.A., M.F.H., T.C.-G.; Visualization: T.C.-G.; Supervision: L.O.A., M.F.H., T.C.-G.; Project administration: M.F.H., T.C.-G.; Funding acquisition: M.F.H., T.C.-G.

Funding

This work received support from Conselho Nacional de Desenvolvimento Científico e Tecnológico (CNPq) and Fundação de Amparo à Pesquisa de Minas Gerais (FAPEMIG). V.S.C.-C. was a FAPEMIG fellow and T.C.-G. was a Coordenação de Aperfeiçoamento de Pessoal de Nível Superior (CAPES) fellow.

Supplementary information

Supplementary information available online at
http://jcs.biologists.org/lookup/doi/10.1242/jcs.226183.supplemental

References

Andrews, N. W., Corrotte, M. and Castro-Gomes, T. (2015). Above the fray: Surface remodeling by secreted lysosomal enzymes leads to endocytosis-mediated plasma membrane repair. *Semin. Cell Dev. Biol.* **45**, 10-17.

Bennett, C. L., Misslitz, A., Colledge, L., Aebischer, T. and Blackburn, C. C. (2001). Silent infection of bone marrow-derived dendritic cells by Leishmania mexicana amastigotes. *Eur. J. Immunol.* **31**, 876-883.

Besteiro, S., Dubremetz, J.-F. and Lebrun, M. (2011). The moving junction of apicomplexan parasites: a key structure for invasion. *Cell. Microbiol.* **13**, 797-805.

Bogdan, C., Donhauser, N., Döring, R., Röllinghoff, M., Diefenbach, A. and Rittig, M. G. (2000). Fibroblasts as host cells in latent leishmaniosis. *J. Exp. Med.* **191**, 2121-2130.

Burza, S., Croft, S. L. and Boelaert, M. (2018). Leishmaniasis. *The Lancet* **392**, 951-970.

Carneiro, M. B. H., Roma, E. H., Ranson, A. J., Doria, N. A., Debrabant, A., Sacks, D. L., Vieira, L. Q. and Peters, N. C. (2018). NOX2-derived reactive oxygen species control inflammation during *Leishmania amazonensis* infection by mediating infection-induced neutrophil apoptosis. *J. Immunol.* **200**, 196-208.

Castro-Gomes, T., Almeida-Campos, F. R., Calzavara-Silva, C. E., da Silva, R. A., Frézard, F. and Horta, M. F. (2009). Membrane binding requirements for the cytolytic activity of *Leishmania amazonensis* leishporin. *FEBS Lett.* **583**, 3209-3214.

Collot, M., Louvard, D. and Singer, S. J. (1984). Lysosomes are associated with microtubules and not with intermediate filaments in cultured fibroblasts. *Proc. Natl. Acad. Sci. USA* **81**, 788-792.

Couto, N. F., Pedersane, D., Rezende, L., Dias, P. P., Corbani, T. L., Bentini, L. C., Oliveira, A. C. S., Kelles, L. F., Castro-Gomes, T. and Andrade, L. O. (2017). LAMP-2 absence interferes with plasma membrane repair and decreases T. cruzi host cell invasion. *PLoS Negl. Trop. Dis.* **11**, e0005657.

Dramsi, S. and Cossart, P. (2003). Listeriolysin O-mediated calcium influx potentiates entry of Listeria monocytogenes into the human Hep-2 epithelial cell line. *Infect. Immun.* **71**, 3614-3618.

Encarnação, M., Espada, L., Escrevente, C., Mateus, D., Ramalho, J., Michelet, X., Santarino, I., Hsu, V. W., Brenner, M. B., Barral, D. C. et al. (2016). A Rab3a-dependent complex essential for lysosome positioning and plasma membrane repair. *J. Cell Biol.* **213**, 631-640.

Fernandes, M. C., Cortez, M., Flannery, A. R., Tam, C., Mortara, R. A. and Andrews, N. W. (2011). *Trypanosoma cruzi* subverts the sphingomyelinase-mediated plasma membrane repair pathway for cell invasion. *J. Exp. Med.* **208**, 909-921.

Forestier, C.-L., Machu, C., Loussert, C., Pescher, P. and Späth, G. F. (2011). Imaging host cell-Leishmania interaction dynamics implicates parasite motility, lysosome recruitment, and host cell wounding in the infection process. *Cell Host Microbe* **9**, 319-330.

Hissa, B., Pontes, B., Roma, P. M. S., Alves, A. P., Rocha, C. D., Valverde, T. M., Aguiar, P. H. N., Almeida, F. P., Guimarães, A. J., Guatimosim, C. et al. (2013). Membrane cholesterol removal changes mechanical properties of cells and induces secretion of a specific pool of lysosomes. *PLoS One* **8**, e82988.

Holbrook, T. W. and Palczuk, N. C. (1975). Leishmania in the chick embryo. IV. Effects of embryo age and hatching, and behavior of L. donovani in cultures of chick fibroblasts. *Exp. Parasitol.* **37**, 398-404.

Idone, V., Tam, C., Goss, J. W., Toomre, D., Pypaert, M. and Andrews, N. W. (2008). Repair of injured plasma membrane by rapid Ca^{2+}-dependent endocytosis. *J. Cell Biol.* **180**, 905-914.

Laskay, T., van Zandbergen, G. and Solbach, W. (2003). Neutrophil granulocytes – Trojan horses for Leishmania major and other intracellular microbes? *Trends Microbiol.* **11**, 210-214.

Luo, J., Zhu, Y., Zhu, M. X. and Hu, H. (2011). Cell-based calcium assay for medium to high throughput screening of TRP channel functions using FlexStation 3. *J. Vis. Exp*, **54**, e149.

Minero, M. A., Chinchilla, M., Guerrero, O. M. and Castro, A. (2004). [Infection of skin fibroblasts in animals with different levels of sensitivity to Leishmania infantum and Leishmania mexicana (Kinetoplastida: Trypanosomatidae)]. *Rev. Biol. Trop.* **52**, 261-267.

Nabavi, N., Urukova, Y., Cardelli, M., Aubin, J. E. and Harrison, R. E. (2008). Lysosome dispersion in osteoblasts accommodates enhanced collagen production during differentiation. *J. Biol. Chem.* **283**, 19678-19690.

Noronha, F. S. M., Cruz, J. S., Beirão, P. S. L. and Horta, M. F. (2000). Macrophage damage by Leishmania amazonensis cytolysin: evidence of pore formation on cell membrane. *Infect. Immun.* **68**, 4578-4584.

Pace, J., Hayman, M. J. and Galán, J. E. (1993). Signal transduction and invasion of epithelial cells by S. *typhimurium. Cell* **72**, 505-514.

Peters, N. C., Egen, J. G., Secundino, N., Debrabant, A., Kimblin, N., Kamhawi, S., Lawyer, P., Fay, M. P., Germain, R. N. and Sacks, D. (2008). In vivo imaging reveals an essential role for neutrophils in leishmaniasis transmitted by sand flies. *Science (80-.)* **321**, 970-974.

Reddy, A., Caler, E. V. and Andrews, N. W. (2001). Plasma membrane repair is mediated by Ca(2+)-regulated exocytosis of lysosomes. *Cell* **106**, 157-169.

Rittig, M. G. and Bogdan, C. (2000). Leishmania-host-cell interaction: complexities and alternative views. *Parasitol. Today* **16**, 292-297.

Rodríguez, A., Samoff, E., Rioult, M. G., Chung, A. and Andrews, N. W. (1996a). Host cell invasion by trypanosomes requires lysosomes and microtubule/kinesin-mediated transport. *J. Cell Biol.* **134**, 349-362.

Rodríguez, J. H., Mozos, E., Méndez, A., Pérez, J. and Gómez-Villamandos, J. C. (1996b). Leishmania infection of canine skin fibroblasts in vivo. *Vet. Pathol.* **33**, 469-473.

Rodríguez, A., Webster, P., Ortego, J. and Andrews, N. W. (1997). Lysosomes behave as Ca^{2+}-regulated exocytic vesicles in fibroblasts and epithelial cells. *J. Cell Biol.* **137**, 93-104.

Schettino, P. M. S., Majumder, S. and Kierszenbaum, F. (1995). Regulatory effect of the level of free Ca2+ of the host cell on the capacity of Trypanosoma cruzi to invade and multiply intracellularly. *J. Parasitol.* **81**, 597-602.

Schille, S., Crauwels, P., Bohn, R., Bagola, K., Walther, P. and van Zandbergen, G. (2018). LC3-associated phagocytosis in microbial pathogenesis. *Int. J. Med. Microbiol.* **308**, 228-236.

Schwartzman, J. D. and Pearson, R. D. (1985). The interaction of Leishmania donovani promastigotes and human fibroblasts in vitro. *Am. J. Trop. Med. Hyg.* **34**, 850-855.

Shaw, T. J. and Martin, P. (2016). Wound repair: a showcase for cell plasticity and migration. *Curr. Opin. Cell Biol.* **42**, 29-37.

Smith, R. S., Smith, T. J., Blieden, T. M. and Phipps, R. P. (1997). Fibroblasts as sentinel cells. Synthesis of chemokines and regulation of inflammation. *Am. J. Pathol.* **151**, 317-322.

Soares, R. P. P., Macedo, M. E., Ropert, C., Gontijo, N. F., Almeida, I. C., Gazzinelli, R. T., Pimenta, P. F. P. and Turco, S. J. (2002). Leishmania chagasi: lipophosphoglycan characterization and binding to the midgut of the sand fly vector Lutzomyia longipalpis. *Mol. Biochem. Parasitol.* **121**, 213-224.

Späth, G. F. and Beverley, S. M. (2001). A lipophosphoglycan-independent method for isolation of infective leishmania metacyclic promastigotes by density gradient centrifugation. *Exp. Parasitol.* **99**, 97-103.

Tam, C., Idone, V., Devlin, C., Fernandes, M. C., Flannery, A., He, X., Schuchman, E., Tabas, I. and Andrews, N. W. (2010). Exocytosis of acid sphingomyelinase by wounded cells promotes endocytosis and plasma membrane repair. *J. Cell Biol.* **189**, 1027-1038.

Tardieux, I., Webster, P., Ravesloot, J., Boron, W., Lunn, J. A., Heuser, J. E. and Andrews, N. W. (1992). Lysosome recruitment and fusion are early events required for trypanosome invasion of mammalian cells. *Cell* **71**, 1117-1130.

Tardieux, I., Nathanson, M. H. and Andrews, N. W. (1994). Role in host cell invasion of Trypanosoma cruzi-induced cytosolic-free Ca2+ transients. *J. Exp. Med.* **179**, 1017-1022.

Valentin-Weigand, P., Jungnitz, H., Zock, A., Rohde, M. and Chhatwal, G. S. (1997). Characterization of group B streptococcal invasion in HEp-2 epithelial cells. *FEMS Microbiol. Lett.* **147**, 69-74.

van Zandbergen, G., Solbach, W. and Laskay, T. (2007). Apoptosis driven infection. *Autoimmunity* **40**, 349-352.

Xu, Y. and Weiss, L. M. (2005). The microsporidian polar tube: a highly specialised invasion organelle. *Int. J. Parasitol.* **35**, 941-953.